Magnetic Resonance in Medicine 47:736–741 (2002)
DOI 10.1002/mrm.10117

Comparison of Diffusion-Weighted High-Resolution CBF and Spin-Echo BOLD fMRI at 9.4 T

Sang-Pil Lee, Afonso C. Silva, and Seong-Gi Kim*

The quantification of blood oxygenation-level dependent (BOLD) functional MRI (fMRI) signals is closely related to cerebral blood flow (CBF) change; therefore, understanding the exact relationship between BOLD and CBF changes on a pixel-by-pixel basis is fundamental. In this study, quantitative CBF changes induced by neural activity were used to quantify BOLD signal changes during somatosensory stimulation in α-chloralose-anesthetized rats. To examine the influence of fast-moving vascular spins in quantifying CBF, bipolar gradients were employed. Our data show no significant difference in relative CBF changes obtained with and without bipolar gradients. To compare BOLD and CBF signal changes induced by neural stimulation, a spin-echo (SE) sequence with long SE time of 40 ms at 9.4 T was used in conjunction with an arterial spin labeling technique. SE BOLD changes were quantitatively correlated to CBF changes on a pixel-by-pixel and animal-by-animal basis. Thus, SE BOLD-based fMRI at high magnetic fields allows a quantitative comparison of functional brain activities across brain regions and subjects. Magn Reson Med 47: 736–741, 2002. © 2002 Wiley-Liss, Inc.

Key words: functional brain mapping; BOLD; arterial spin labeling; rat brain; forepaw stimulation; high resolution; high field

In the intact brain, neuronal activation is closely coupled to an increase of cerebral blood flow (CBF) and metabolic activity (1). Regional CBF change induced by local neuronal activity is known to be localized to a submillimeter columnar level (2), and has been widely used to detect functionally active regions in the brain (3,4). Recently developed arterial spin-labeling MRI techniques allow noninvasive assessments of CBF (5–7). CBF-weighted MRI signals consist of tissue/capillary and arterial vascular components. The contribution of large arterial vessels to CBF-weighted signals can be up to 50% (8,9), inducing an overestimation of absolute CBF. Therefore, it is important to investigate quantification errors of relative CBF changes during neural activation due to the contributions of arterial blood vessels.

Because of its high contrast-to-noise ratio (CNR) and simplicity of implementation, blood oxygenation-level dependent (BOLD) functional MRI (fMRI) is the most widely used brain mapping technique. BOLD contrast is very sensitive to susceptibility changes within and around large draining veins, especially in gradient-echo (GE) based fMRI techniques (10). Pixels with high GE BOLD percent changes often contain both large draining veins and nearby tissue without significant CBF changes. Thus, BOLD percent changes are not correlated to the magnitude of CBF changes in those pixels (11–13). This results in poor correlation between CBF changes and corresponding BOLD signal changes at high spatial resolution (11,13). Therefore, quantitative interpretation of BOLD percent changes across pixels, regions, and subjects is difficult. When a spin-echo (SE) technique with a TE much longer than T_2 of venous blood is used, vascular contributions can be reduced by minimizing extra- and intravascular contributions from large veins. At high magnetic fields, such as 9.4 T, the SE-based BOLD signal arises mostly from small vessels, including the capillary bed (14). Even where the contribution of large vessels to the BOLD signal is negligible, BOLD signal changes may not correlate quantitatively with relative CBF changes because the BOLD signal derives from a mismatch between oxygen supply via CBF and oxygen consumption of cerebral tissue. Therefore, a comparison of BOLD with CBF-based fMRI, which provides quantitative flow changes localized in brain parenchyma (11,12), is needed to provide further insight into the signal sources of the BOLD contrast, and to quantify SE BOLD signals.

In the present study, to further examine the effect of large-vessel contributions to CBF signals measured during resting and elevated CBF, diffusion-weighted bipolar gradients were employed to reduce fast-moving vascular spins (8,9,15). To compare neural activity-induced BOLD and CBF signal changes on a pixel-by-pixel basis, SE BOLD and CBF images were simultaneously measured during somatosensory stimulation. Our data showed no significant difference in relative CBF changes measured with or without flow-crushing gradients, and an excellent correlation between SE BOLD and CBF-based fMRI.

MATERIALS AND METHODS

Animal Preparation and Stimulation

Ten male Sprague-Dawley rats weighing 250–300 g were prepared as described elsewhere (14,16). To maintain the animals, an initial dose of 80 mg/kg and subsequent doses of 40 mg/kg α-chloralose were administered intravenously every 90 min.

For forepaw stimulation, two pairs of needle electrodes were inserted under the skin of the right and left forepaws and connected to a current stimulator (model S48; Grass, West Warwick, RI) as described previously (14). Either the right or the left forepaw was used for each stimulation epoch. Stimulation parameters were optimized previously

Center for Magnetic Resonance Research, Department of Radiology, University of Minnesota Medical School, Minneapolis, Minnesota.

Grant sponsor: National Institute of Health; Grant numbers: RR08079; NS38295; NS40719; Grant sponsor: Keck Foundation.

S.-P. Lee's present address is Nathan S. Kline Institute, 140 Old Orangeburg Road, Orangeburg, NY 10962.

A.C. Silva's present address is Laboratory of Functional and Molecular Imaging, National Institute of Neurological Disorders and Stroke, National Institutes of Health, Bethesda, MD 20892.

*Correspondence to: Seong-Gi Kim, Ph.D., Center for Magnetic Resonance Research, University of Minnesota Medical School, 2021 Sixth Street SE, Minneapolis, MN 55455. E-mail: kim@cmrr.umn.edu

Received 13 March 2001; revised 4 December 2001; accepted 10 December 2001.

(16) to produce robust CBF changes without any nonspecific systemic changes in blood pressure: a current of 1.5 mA, pulse duration of 0.3 ms, and repetition rate of 3 Hz were used. The stimulation paradigm consisted of 2 min of rest, 1 min of forepaw stimulation, and 2 min of rest conditions. To ensure reproducible responses in multiple trials, each experiment was separated by a resting period of at least 10 min.

MRI Measurements

All MRI measurements were performed on a 9.4 T horizontal magnet equipped with an actively shielded gradient insert (11 cm inner diameter) operating at a maximum gradient strength of 300 mT/m and a slew rate of 1000 T/m/s (Magnex, Abingdon, UK), and interfaced to a Unity INOVA console (Varian, Palo Alto, CA). A surface (imaging) coil of 1.6 cm diameter was positioned on top of the rat's head, and a butterfly-shaped spin-tagging coil of 0.8 cm inner diameter was placed underneath the neck. The two coils were geometrically decoupled to provide an electrical isolation greater than 20 dB. Multislice fast low-angle shot (FLASH) images were acquired to identify the anatomical structures in the brain and to position the slice of interest in the isocenter of the magnetic field.

fMRI studies were performed using a single-shot, double SE, echo-planar imaging (EPI) sequence implemented with bipolar gradients for diffusion weighting (14). This technique enabled the use of a surface coil for RF excitation and detection with maximal sensitivity for SE images. Imaging parameters were: data matrix = 64 × 32, field of view (FOV) = 3.0 cm × 1.5 cm, slice-thickness = 2 mm, and repetition time (TR) = ~3 s. Data acquisition was synchronized to the breathing cycle by adjusting the TR to be a multiple of the respiratory period, which was controlled by a pressure-driven ventilator (Kent Scientific, Litchfield, CT). Echo time (TE) was set to 40 ms for a maximum sensitivity of BOLD contrast at 9.4 T (14). A single coronal slice covering the forelimb area of the primary somatosensory cortex was selected as the best responding slice, as determined by scout multislice fMRI using a GE EPI sequence.

Control and arterial spin tagged images were acquired in an alternate manner, resulting in actual temporal resolution of ~6 s. Arterial spins were labeled according to the principle of adiabatic fast passage (17) using continuous irradiation of RF with a butterfly-shaped neck coil in the presence of a 10 mT/m longitudinal gradient. The time for arterial spin labeling was set to ~3 s to allow the build-up of a steady-state perfusion contrast in the imaging plane.

Contribution of Vascular Spins to CBF Signals

To investigate the vascular signal contribution to CBF measurement, diffusion-sensitizing bipolar gradients were applied between the two refocusing 180° RF pulses in the double SE EPI sequence (14). Typical values for the diffusion-weighting parameters used in this study were: inter-gradient separation = 10 ms, and gradient duration = 5–8 ms. Diffusion weighting was achieved up to *b*-values of 500 s/mm^2 by adjusting the gradient strength up to 180 mT/m. Gradients were applied along the longitudinal (z) direction. A *b*-value of 500 s/mm^2 is sufficient to eliminate signals from arterial vessels and significantly reduce signals from all other intravascular compartments (18,19). Then, quantitative CBF maps during control and stimulation periods were separately computed on a pixel-by-pixel basis using a formula described previously (16). Relative CBF changes in fMRI studies with various *b*-values were determined from the same region of interest (ROI) for comparison. Two ROIs, 9 and 25 pixels each, were chosen from the center of the active area, which was located at the contralateral somatosensory cortex. All averaged data were reported by means and their standard deviations.

Comparison of CBF and Spin-Echo BOLD Signals

CBF and BOLD functional maps were calculated from CBF and control images obtained in the same stimulation session using a boxcar cross-correlation method. Relative signal changes of CBF and BOLD fMRI were calculated in pixels with a statistical significance level, *t*-value, of greater than 3.8 ($P = 0.002$). The *t*-values and relative signal changes of CBF and BOLD fMRI were compared on a pixel-by-pixel basis.

The relationship between BOLD signal and CBF changes was further characterized with a biophysical model (10,20). Assuming the effect of venous blood volume changes on the BOLD signals is negligible (19) compared to that of venous oxygenation changes (Δy), relative BOLD signal changes (*BOLD*) can be approximated as:

$$BOLD \approx \alpha^* \cdot TE \cdot \Delta y, \quad [1]$$

where α^* is a constant dependent mainly on venous blood volume and static magnetic field strength. In addition, a linear relationship between relative changes in the oxygen consumption rate ($CMRO_2$) and CBF during neural stimulation, $k = \Delta rCMRO_2/\Delta rCBF$, is assumed based on recent experimental data and theoretical modeling of cerebral oxygen delivery (20–22). This assumption differs from a model by Buxton et al. (23), which predicts a nonlinear relationship between $\Delta rCMRO_2$ and $\Delta rCBF$. Using the mass conservation law on oxygen, $CMRO_2 = (1 - y) \cdot CBF$ assuming an arterial oxygenation level of 1.0, Δy can be expressed in terms of $\Delta rCBF$ and k. The relationship between BOLD and $\Delta rCBF$ is then

$$BOLD \approx \alpha^* TE(1 - y_0)(1 - k)\frac{\Delta rCBF}{1 + \Delta rCBF} = A \cdot TE \cdot \frac{\Delta rCBF}{1 + \Delta rCBF}, \quad [2]$$

where y_0 is the basal venous oxygenation level and A is a constant defined as $A = \alpha^* \cdot (1 - y_0) \cdot (1 - k)$. Relative CBF and BOLD signal changes were fitted using Eq. [2].

RESULTS

Contribution of Vascular Spins to CBF Signals

Twelve stimulation studies in 10 animals were performed with various diffusion-weighted gradients to examine the dependence of rCBF changes during neural activation on

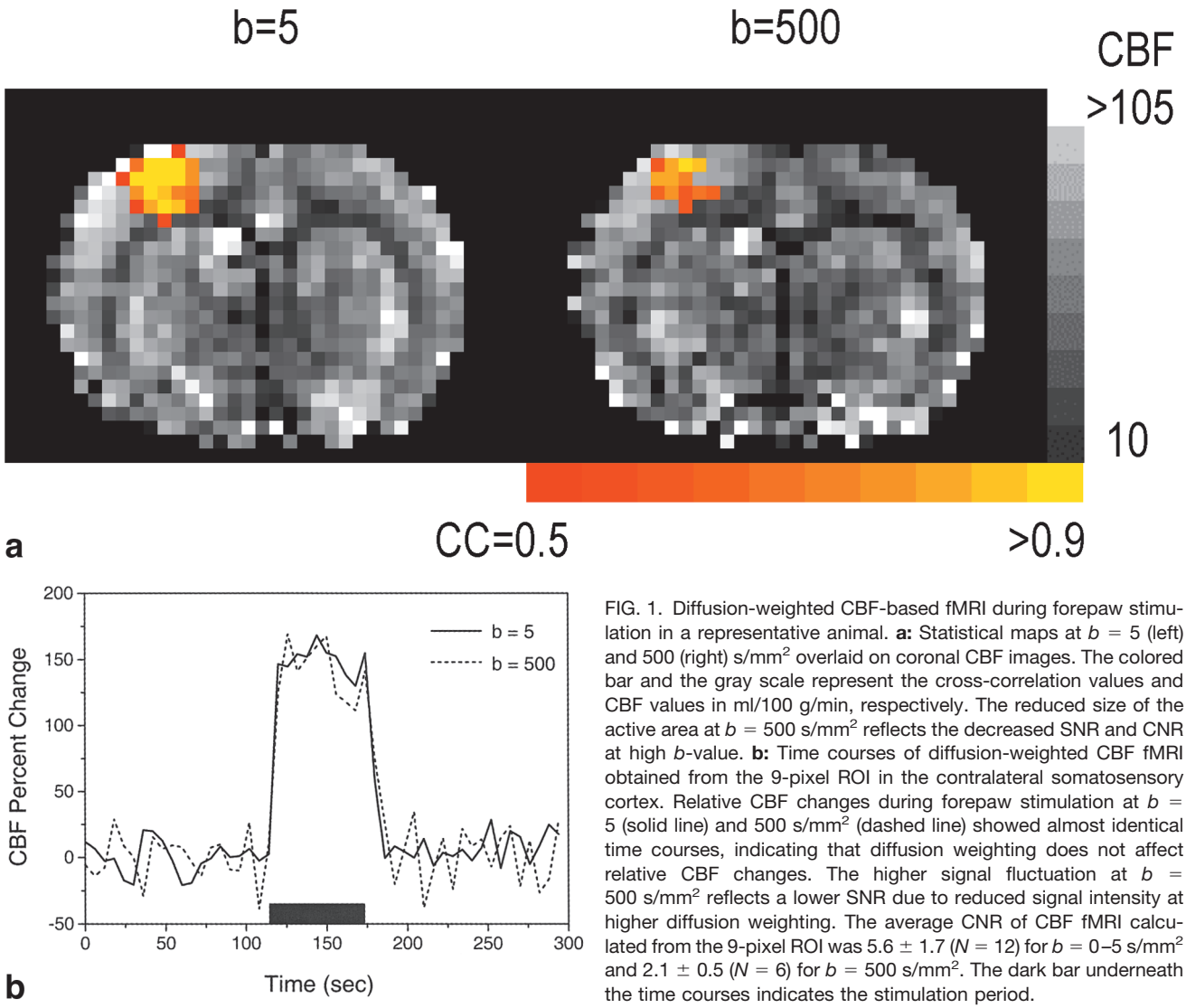

FIG. 1. Diffusion-weighted CBF-based fMRI during forepaw stimulation in a representative animal. **a:** Statistical maps at $b = 5$ (left) and 500 (right) s/mm^2 overlaid on coronal CBF images. The colored bar and the gray scale represent the cross-correlation values and CBF values in ml/100 g/min, respectively. The reduced size of the active area at $b = 500$ s/mm^2 reflects the decreased SNR and CNR at high b-value. **b:** Time courses of diffusion-weighted CBF fMRI obtained from the 9-pixel ROI in the contralateral somatosensory cortex. Relative CBF changes during forepaw stimulation at $b = 5$ (solid line) and 500 s/mm^2 (dashed line) showed almost identical time courses, indicating that diffusion weighting does not affect relative CBF changes. The higher signal fluctuation at $b = 500$ s/mm^2 reflects a lower SNR due to reduced signal intensity at higher diffusion weighting. The average CNR of CBF fMRI calculated from the 9-pixel ROI was 5.6 ± 1.7 ($N = 12$) for $b = 0$–5 s/mm^2 and 2.1 ± 0.5 ($N = 6$) for $b = 500$ s/mm^2. The dark bar underneath the time courses indicates the stimulation period.

vascular contribution. Figure 1a shows cross-correlation maps of CBF fMRI obtained during electrical stimulation of the rat forepaw at low (left) and high (right) diffusion weightings overlaid on the corresponding basal quantitative CBF images. Very high basal CBF values on the order of 200 ml/100 g/min were observed in some pixels partly due to contribution from large arterial vessels and low signal-to-noise ratio (SNR). The average CBF value obtained from the entire slice at $b = 5$ s/mm^2 was 61 ml/100 g/min (Fig. 1a). When a b-value of 500 s/mm^2 was applied, the average CBF in the entire slice was reduced to 52 ml/100 g/min (Fig. 1a). Similarly, when only the cortical area or the 9-pixel ROI was used in this analysis, the CBF reduction of 10–15% due to bipolar gradients was observed. Results obtained from all of the animals were consistent.

Activation in both low and high b-value fMRI studies is located in the forelimb area of the contralateral somatosensory cortex. The highest CBF change was observed in the middle of the cortex (cortical layer IV), not at the surface of the cortex. The size of the active region is reduced and the cross-correlation values are decreased at higher diffusion weighting ($b = 500$ s/mm^2) due to the decreased CNR and SNR of the image. The average absolute CBF increase (at low b-value data) in the 9-pixel ROI was 111 ± 28 ml/100 g/min ($N = 12$ paws) from its basal value of 80 ± 15 ml/100 g/min, corresponding to a relative CBF percent change of 146 ± 35%.

Figure 1b shows the time courses of the relative CBF changes obtained from the same 9 pixels at the center of the active region in Fig. 1a. The higher signal fluctuation of the CBF trace at $b = 500$ s/mm^2 is indicative of the reduced SNR at a larger diffusion weighting. No significant differences in relative CBF signal changes between the two time courses were observed. Also, in both the 9-pixel and the 25-pixel ROIs, there were no statistically significant changes in the relative CBF increases induced by stimulation at different b-values.

Comparison of CBF and Spin-Echo BOLD fMRI

Relative BOLD and CBF signal changes during forepaw stimulation were compared on a pixel-by-pixel manner in a representative animal (Fig. 2). Two sets of data acquired

90 min apart (shown in diamonds and circles) show good reproducibility. Statistically significant levels (*t*-values) of SE BOLD and CBF fMRI data show an excellent correlation (Fig. 2a), and the slope of a linear regression curve is 1.006 ($P < 0.001$). The values of CNR obtained from the 9-pixel ROI in the fMRI data with low *b*-values of 0–5 s/mm^2, defined as (signal change)/(fluctuation of baseline), were 5.6 ± 1.7 and 5.7 ± 1.6 ($N = 12$) for CBF and BOLD fMRI, respectively. A good correlation between relative BOLD and CBF changes was also observed for individual pixels (Fig. 2b).

Figure 3 shows the relationship between relative BOLD and CBF changes obtained from 9-pixel ROIs across various measurements. Individual diffusion-weighted fMRI data obtained from 10 animals (12 paws) were plotted; low diffusion gradient data ($b = 0–5$ s/mm^2) are shown as circles, intermediate ($b = 20–100$ s/mm^2) as squares, and high ($b = 150–500$ s/mm^2) as triangles. The relationship between relative BOLD and CBF changes was identical in all groups, indicating that the presence of diffusion-weighting gradients did not affect any signal. When all the data obtained at various diffusion weightings were analyzed without distinguishing *b*-values, they were best fitted to BOLD = A × TE × ΔrCBF/(1 + ΔrCBF) = 2.3 × 0.04 × ΔrCBF/(1 + ΔrCBF), which is the same as that obtained from many pixels in one animal (Fig. 2b). For comparison, in the previous GE BOLD data *A* was found to be 7.7 s^{-1} (16,24), which is higher than that in the SE data (2.3 s^{-1}).

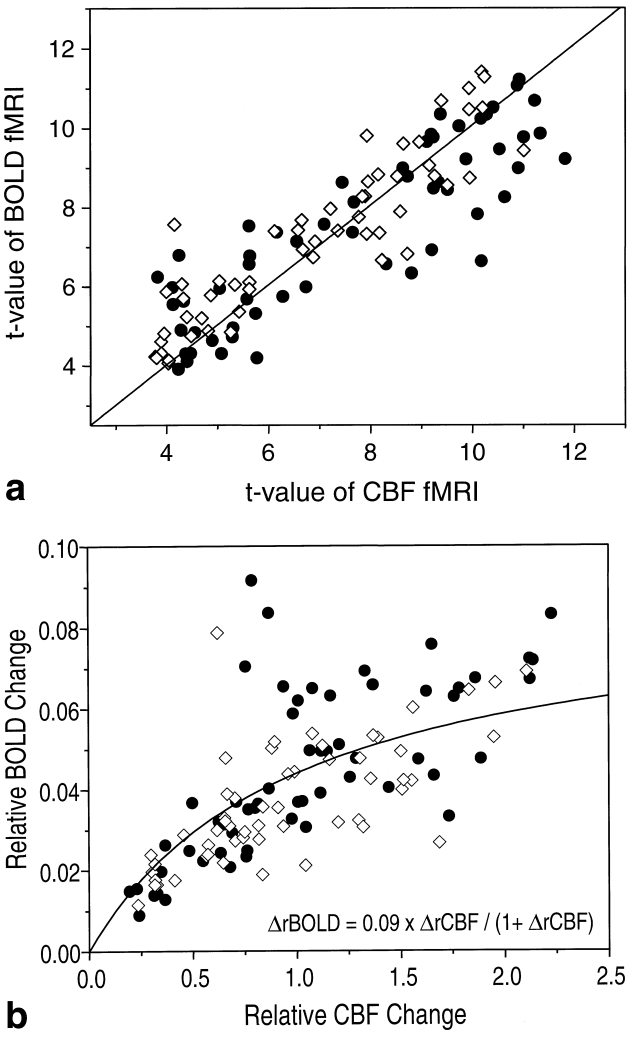

FIG. 2. Comparison of SE BOLD and CBF fMRI on a pixel-by-pixel basis. Filled circles and open diamonds represent the data acquired 90 min apart at $b = 0$ and $b = 2$ s/mm^2, respectively. Excellent reproducibility was observed. **a:** Correlation between *t*-values of BOLD and CBF fMRI. Pixels were selected by thresholding a *t*-value of 3.8 ($P = 0.002$). A fitted line indicates the linear regression line with a slope of 1.006 ($P < 0.001$). **b:** Correlation between relative BOLD and relative CBF changes. Relative fMRI signal changes were obtained from the same data used in **a**. A solid line indicates the best-fitted curve with Eq. [2].

DISCUSSION

Vascular Contribution to CBF

Absolute CBF values, obtained without crushing out the arterial vascular component, are overestimated by 10–15%. This observation is consistent with a previous CBF study performed in rats at 4.7 T, in which 10–20% of the signal was reduced when a *b*-value of 20 s/mm^2 was applied (9). Assuming no changes in the arterial vascular volume during increased CBF, it is expected that relative CBF changes without bipolar gradients would be systematically underestimated. However, the observation that relative CBF change remains constant, regardless of the strength of bipolar gradients, suggests that the arterial blood vessels including arterioles dilate proportionally to the CBF changes. This is consistent with our previous finding of significant arterial CBV changes during increased CBF (19). In addition, the small overall reduction in resting CBF values due to diffusion weighting can be considered insignificant compared to the relative CBF signal changes induced by functional activation (on the order of 150% in the current study and 125% in our previous study (16)). Taken together, the contribution of large vessels to functional CBF changes, as measured by the continuous arterial spin labeling technique, does not alter tissue-level relative CBF changes.

Comparison of Spin-Echo BOLD and CBF fMRI

CBF-based fMRI can provide better-localized mapping of neuronal activation because it is not sensitive to large draining vessels. This improved spatial specificity was also observed in our SE BOLD images that were devoid of large arterial and/or venous artifacts (14). Both CBF- and SE BOLD-based fMRI at 9.4 T yield tissue-specific maps. However, since the BOLD contrast is dependent on various physiological and anatomical parameters, it is important to compare the BOLD contrast with CBF-based fMRI, which can play the role of a "gold standard" for measuring a neurally activated area. Our results show excellent correlation between SE BOLD and CBF changes during functional stimulation at the single-pixel level, 470 × 470 μm^2. This is consistent with previous observations that the SE BOLD contrast has its origin in extravascular dynamic averaging effects around small vessels (14). The CBF contrast mostly reflects truly perfusing spins that have perme-

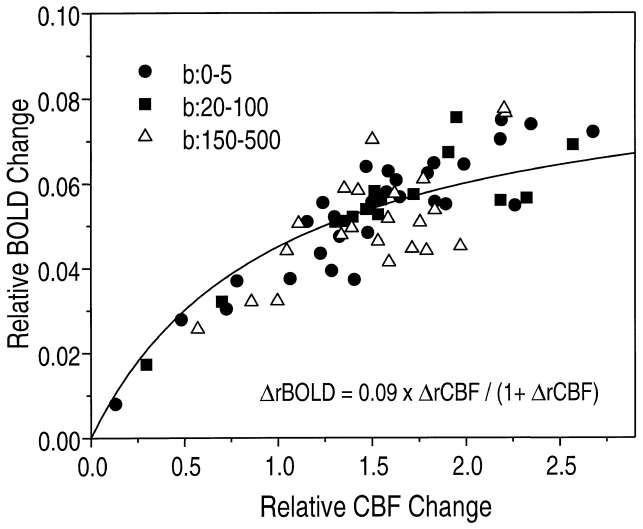

FIG. 3. Comparison of relative BOLD (rBOLD) and relative CBF (rCBF) signal changes obtained from all animals. A 9-pixel ROI was chosen from the contralateral somatosensory cortex. All diffusion-weighted fMRI data obtained from 10 animals (12 paws) were grouped into three diffusion-weighting ranges, $b = 0–5$ s/mm^2, $b = 20–100$ s/mm^2, and $b = 150–500$ s/mm^2. No difference in correlations between BOLD and CBF changes obtained with different diffusion weightings was observed. The solid curve represents a best fit of the data with a model function, Eq. [2], on all data points.

ated the capillary walls and entered the extravascular space (2,5). Both CBF and BOLD fMRI contrasts are closely coupled when the large vascular component is suppressed, and originate from the similar anatomical location within a single voxel. Since relative CBF changes are linearly correlated to metabolic changes (1,25), SE BOLD signal changes can also be used to indicate the strength of metabolic activity in the brain. Thus, SE BOLD-based fMRI at high magnetic fields is a quantitative method for mapping functional brain activity, allowing comparisons across different regions and subjects.

This finding may not apply to the GE BOLD technique. Although intravascular signal can be attenuated significantly with diffusion weighting, large vascular contribution—especially the extravascular contribution of large veins—in GE BOLD-based fMRI cannot be eliminated (14). Tissue areas near large draining veins will have very high GE BOLD changes (10,11,26) without the corresponding tissue blood flow change. Therefore, relative GE BOLD signal changes cannot be used to quantitatively characterize metabolic (and CBF) activities across pixels (14). It should be noted that the relative changes of GE BOLD and CBF signals showed a good correlation in an area *devoid of large vessels* and/or in a large ROI. But avoiding large vessel areas is not straightforward, and thus the best approach is to eliminate large vascular contributions during data acquisition.

Relative BOLD and CBF changes during neural stimulation have been successfully fitted on a wide range of CBF changes using a simple version of an existing biophysical model (10). This suggests that a linear relation between $CMRO_2$ and CBF changes is a reasonable assumption (20,21,27). However, considering the oxygen transport mechanism from capillaries to tissues (22,23), the proportional coefficient, k, could be dependent on blood flow rate and reduced especially at high blood flow. When this modification was included in Eq. [2], the fitting of the data was improved. Note that we cannot accurately determine k due to unknown α^* and basal venous oxygenation level, y_0. However, if we assume α^* obtained in humans at 4 T (28) can be extrapolated to 9.4 T with the quadratic magnetic field dependence, α^* is estimated to be 17.8 s^{-1}, resulting in $k = 0.68$, 0.57, and 0.36 at y_0 of 0.6, 0.7, and 0.8, respectively. Another term to be considered in the model is the CBV change. Inclusion of the CBV change in the equation reduced the goodness of the fit, indicating that the CBV change is not a significant factor in the SE BOLD signal changes. This observation is consistent with our previous study, which showed that venous CBV changes are very small compared to arterial CBV changes during increased CBF (19).

The relationship between the relative BOLD and relative CBF changes measured on anesthetized animals may not be simply extended to awake humans. It has been reported that α-chloralose anesthesia reduces the baseline metabolic rate of glucose (CMR_{glc}) and CBF dramatically by ~65% compared to the awake condition, while it does not alter those in stimulated conditions (3,29,30). In this case, rCBF changes during neural activities would be much greater than those in an awake condition, resulting in an alteration of A in Eq. [2]. Therefore, care should be taken when the results from anesthetized animals are extended to awake conditions (as in most human experiments). Nevertheless, we expect to observe a similar trend of excellent correlation between SE BOLD and CBF at high magnetic fields in humans. However, at low magnetic fields, SE BOLD signal originates predominantly from intravascular water (31); thus, a poor correlation is expected between CBF and SE BOLD at high spatial resolution.

CONCLUSIONS

The SE BOLD technique with long TE at high magnetic fields can be an excellent approach to obtaining quantitative information about functional brain activity, with high spatial specificity. Thus, SE BOLD-based fMRI at high magnetic fields can be used to compare functional brain activities among different pixels and across different subjects. Furthermore, the T_2-based MRI technique at high magnetic fields can be used to obtain submillimeter resolution fMRI in animals and humans.

ACKNOWLEDGMENTS

The authors thank Drs. Hellmut Merkle and Gregor Adriany for hardware support, and Ms. Chardonnay J. Vance for her careful reading of this manuscript. The 9.4 T facility was funded in part by the Keck Foundation.

REFERENCES

1. Sokoloff L, Reivich M, Kennedy C, Des Rosiers M, Patlak G, Pettigrew K, Sakurada O, Shinohara M. The [14C] deoxyglucose method for the measurement of local cerebral glucose utilization: theory, procedure, and normal values in the conscious and anesthetized albino rat. J Neurochem 1977;28:897–916.

2. Duong TQ, Kim DS, Ugurbil K, Kim SG. Localized cerebral blood flow response at submillimeter columnar resolution. Proc Natl Acad Sci USA 2001;98:10904–10909.
3. Ueki M, Miles G, Hossmann K-A. Effect of alpha-cloralose, halothane, pentobarbital and nitrous oxide anesthesia on metabolic coupling in somatosensory cortex of rat. Acta Anaesthesiol Scand 1992;36:318–322.
4. Raichle ME. Food for thought. The metabolic and circulatory requirements of cognition. Ann NY Acad Sci 1997;835:373–385.
5. Detre JA, Leigh JS, Williams DS, Koretsky AP. Perfusion imaging. Magn Reson Med 1992;23:37–45.
6. Kwong KK, Chesler DA, Weisskoff RM, Donahue KM, Davis TL, Ostergaard L, Campbell TA, Rosen BR. MR perfusion studies with T1-weighted echo planar imaging. Magn Reson Med 1995;34:878–887.
7. Kim S-G. Quantification of relative cerebral blood flow change by flow-sensitive alternating inversion recovery (FAIR) technique: application to functional mapping. Magn Reson Med 1995;34:293–301.
8. Ye FQ, Mattay VS, Jezzard P, Frank JA, Weinberger DR, McLaughlin AC. Correction for vascular artifacts in cerebral blood flow values by using arterial spin tagging techniques. Magn Reson Med 1997;37:226–235.
9. Silva A, Williams D, Koretsky A. Evidence for the exchange of arterial spin-labeled water with tissue water in rat brain from diffusion-sensitized measurements of perfusion. Magn Reson Med 1997;38:232–237.
10. Ogawa S, Menon RS, Tank DW, Kim SG, Merkle H, Ellermann JM, Ugurbil K. Functional brain mapping by blood oxygenation level-dependent contrast magnetic resonance imaging. A comparison of signal characteristics with a biophysical model. Biophys J 1993;64:803–812.
11. Kim S-G, Tsekos NV, Ashe J. Multi-slice perfusion-based functional MRI using the FAIR technique: comparison of CBF and BOLD effects. NMR Biomed 1997;10:191–196.
12. Wong EC, Buxton RB, Frank LR. Implementation of quantitative perfusion imaging techniques for functional brain mapping using pulsed arterial spin labeling. NMR Biomed 1997;10:237–249.
13. Luh WM, Wong EC, Bandettini PA, Ward BD, Hyde JS. Comparison of simultaneously measured perfusion and BOLD signal increases during brain activation with T(1)-based tissue identification. Magn Reson Med 2000;44:137–143.
14. Lee SP, Silva AC, Ugurbil K, Kim SG. Diffusion-weighted spin-echo fMRI at 9.4 T: microvascular/tissue contribution to BOLD signal changes. Magn Reson Med 1999;42:919–928.
15. Francis ST, Gowland PA, Bowtell RW. Continuous saturation EPI with diffusion weighting at 3.0 T. NMR Biomed 1999;12:440–450.
16. Silva AC, Lee S-P, Yang G, Iadecola C, Kim S-G. Simultaneous blood oxygenation level-dependent and cerebral blood flow functional magnetic resonance imaging during forepaw stimulation in the rat. J Cereb Blood Flow Metab 1999;19:871–879.
17. Dixon WT, Du LN, Faul DD, Gado M, Rossnick S. Projection angiograms of blood labeled by adiabatic fast passage. Magn Reson Med 1986;3:454–462.
18. Duong TQ, Kim SG. In vivo MR measurements of regional arterial and venous blood volume fractions in intact rat brain. Magn Reson Med 2000;43:393–402.
19. Lee SP, Duong TQ, Yang G, Iadecola C, Kim SG. Relative changes of cerebral arterial and venous blood volumes during increased cerebral blood flow: implications for BOLD fMRI. Magn Reson Med 2001;45:791–800.
20. Kim S-G, Rostrup E, Larsson HBW, Ogawa S, Paulson OB. Determination of relative CMRO2 from CBF and BOLD changes: significant increase of oxygen consumption rate during visual stimulation. Magn Reson Med 1999;41:1152–1161.
21. Hoge RD, Atkinson J, Gill B, Crelier GR, Marrett S, Pike GB. Linear coupling between cerebral blood flow and oxygen consumption in activated human cortex. Proc Natl Acad Sci USA 1999;96:9403–9408.
22. Hyder F, Shulman RG, Rothman DL. A model for the regulation of cerebral oxygen delivery. J Appl Physiol 1998;85:554–564.
23. Buxton RB, Frank LR. A model for the coupling between cerebral blood flow and oxygen metabolism during neural stimulation. J Cereb Blood Flow Metab 1997;17:64–72.
24. Duong TQ, Silva AC, Lee S-P, Kim S-G. Functional MRI of calcium-dependent synaptic activity: cross correlation with CBF and BOLD measurements. Magn Reson Med 2000;43:383–392.
25. Fox PT, Raichle ME. Focal physiological uncoupling of cerebral blood flow and oxidative metabolism during somatosensory stimulation in human subjects. Proc Natl Acad Sci USA 1986;83:1140–1144.
26. Bandettini PA, Wong EC. Effects of biophysical and physiologic parameters on brain activation-induced R2* and R2 changes: simulations using a deterministic diffusion model. Int J Imaging Syst Technol 1995;6:133–152.
27. Kida I, Kennan RP, Rothman DL, Behar KL, Hyder F. High-resolution CMR(O2) mapping in rat cortex: a multiparametric approach to calibration of BOLD image contrast at 7 Tesla. J Cereb Blood Flow Metab 2000;20:847–860.
28. Cohen ER, Ugurbil K, Kim S-G. Estimation of relative oxidative metabolic changes during motor activity during graded hypercapnic calibration at 4 Tesla. In: Proceedings of the 9th Annual Meeting of ISMRM, Glasgow, Scotland, 2001. p 1190.
29. Nakao Y, Itoh Y, Kuang TY, Cook M, Jehle J, Sokoloff L. Effects of anesthesia on functional activation of cerebral blood flow and metabolism. Proc Natl Acad Sci USA 2001;98:7593–7598.
30. Shulman RG, Rothman DL, Hyder F. Stimulated changes in localized cerebral energy consumption under anesthesia. Proc Natl Acad Sci USA 1999;96:3245–3250.
31. Oja JM, Gillen J, Kauppinen RA, Kraut M, van Zijl PC. Venous blood effects in spin-echo fMRI of human brain. Magn Reson Med 1999;42:617–626.